Flutter Analysis of Thin Cracked Panels Using the Finite Element Method

Wen-Hwa Chen* and Heng-Chih Lin†
National Tsing Hua University, Hsinchu, Taiwan, China

An assumed hybrid-displacement finite element model is presented to deal with the flutter problems of thin cracked panels. Based on a modified Hamilton's principle for nonconservative systems with relaxed continuity requirements for deflections and normal slopes at the interelement boundary, the aerodynamic properties of rectangular-shaped hybrid crack elements around the crack tip embedded with proper stress singularities are derived. Interelement compatibility conditions are satisfied through the use of a Lagrangian multiplier technique and the assumption of interelement boundary deflections. First, for verification purposes, the flutter analyses of noncracked panels are illustrated. Excellent agreement between the computed results and referenced solutions is observed. To investigate the nature of the fluttering instability, both the divergent- and oscillatory-type fluttering instabilities are discussed in detail. Several typical types of cracked panels found in aeronautical structures in arbitrarily directed supersonic flows are then studied. The influences of crack lengths and flow directions on the evaluation of the critical speed and type of instability are also drawn. Finally, the important role of the hybrid crack element in dealing with flutter problems of thin cracked panels is demonstrated.

Introduction

FLUTTER is a particular type of dynamic aeroelastic phenomenon characterized by the interactions of aerodynamic, elastic, and inertial forces. In fact, when the speed of an airflow is high enough, such an unstable feature is expected once the structure extracts more energy from the airstream than that lost due to the damping of the structure and aerodynamic pressure and is of practical importance in the design of aeronautical structures; the necessity to develop an efficient and accurate numerical procedure that can give reliable prediction of the flutter response is obvious.

The finite element technique, which has been demonstrated as an excellent method for static and dynamic structural analyses, has been introduced by numerous authors to study the flutter behavior of thin panels. Based on the linearized piston theory,[1] the first attempt was made by Olson,[2,3] who succeeded in deriving the aerodynamic matrix for several bending plate elements. The model proposed by Olson[2,3] was then extended by Kariappa et al.[4] and Sander et al.[5] to yawed supersonic flows, and by Kariappa et al.,[4] Rossettos and Tong,[6] and Sawyer[7] to skew, anisotropic, and laminated plates, respectively. Among these approaches and other analytic work[8-10] achieved in literature, however, flutter analyses for cracked panels are still very limited and should receive attention.

Thus, the aim of the present work is to extend the previous applications of the assumed hybrid-displacement finite element model for elastodynamic cracked problems[11-17] to the investigations of the flutter response of cracked panels. The finite element formulation is based on a modified Hamilton's principle for nonconservative systems[18] with relaxed continuity requirements for deflections and normal slopes at the interelement boundary. The interelement compatibility conditions are satisfied in an integral sense through the use of a Lagrangian multiplier technique[19] and the assumption of interelement boundary deflections. The singularity of stresses[20] near the crack tip can be embedded by introducing the symmetric- and antisymmetric-mode bending stress intensity factors, K_I and K_{II}, as generalized parameters. However, for simplicity, the conventional displacement finite element model and conforming bending plate elements are employed for the regions far away from the crack tip. To reduce the size of the final simultaneous homogeneous equations of flutter problems, the modal method,[6] for which only several modes of natural vibrations are chosen to represent the problem, is used before the QR algorithm[21] is performed for determining the eigenvalues.

As is known, the eigenvalues of the flutter problem can be altered by aerodynamic pressure such that two of them may approach each other as the flow speed increases and, thus, coalesce at a critial value.[2,3] Another possible case is that one of the eigenvalues may shrink gradually to zero when the speed approaches its critical value.[22,23] Since the eigenvalues are negative, the disturbance on the structure diverges and causes failure shortly thereafter. In this work, the nature of the fluttering instability is investigated. The influences of crack lengths and flow directions on the evaluation of the critical speed and the type of fluttering instability are then presented. In addition, the role of the aerodynamic damping effect is observed.

For verification purposes, the flutter analyses of noncracked panels are illustrated first. Excellent agreement between the present computed results and referenced solutions[3,5,6] can be found. Several typical types of cracked panels found in aeronautical structures subjected to arbitrarily directed supersonic flows are then solved. Finally, the important role of the hybrid crack element is also assessed.

Theoretical Formulation

From the linearized piston theory,[1] the disturbed aerodynamic pressure p' exerted on a deflected panel at supersonic speeds of Mach number $\gtrsim 1.6$ is related to the deflection w as

$$p' = \frac{2q_\infty}{\sqrt{M^2-1}}\cos\theta\frac{\partial w}{\partial x} + \frac{2q_\infty}{\sqrt{M^2-1}}\sin\theta\frac{\partial w}{\partial y} + \frac{1}{U_\infty}\frac{2q_\infty}{\sqrt{M^2-1}}\frac{M^2-2}{M^2-1}\frac{\partial w}{\partial t} \tag{1}$$

where U_∞ is the freestream velocity, M the Mach number, $q_\infty = \frac{1}{2}\rho_\infty U_\infty^2$ the freestream dynamic pressure, ρ_∞ the density

Received Sept. 15, 1983; revision received May 29, 1984.

*Professor and Head, Department of Power Mechanical Engineering.
†Graduate Student, Department of Power Mechanical Engineering.

of the freestream, and θ the direction angle of the flow speed. It is noted that the first two terms on the right-hand side of Eq. (1) denote the primary part of the disturbed aerodynamic force which governs the phase angles and distortions of mode shapes in supersonic flows. Whereas, the last term, as a secondary part, represents the aerodynamic damping which prevents the instability of out-of-phase oscillation.

The domain of the present cracked panel can be separated into two regions, i.e., the singular and regular regions. In the singular region around the crack tip, the assumed hybrid-displacement model[17] is used to derive the stiffness, aerodynamic, and mass matrices of the hybrid crack elements. While in the regular region, the conventional displacement model is sufficient to derive such matrices of regular elements.

In the singular region, based on the modified Hamilton's principle,[17,18] the variational principle governing the flutter response of thin panels can be shown as $\delta\Pi_{HD}=0$, that is,

$$\delta\Pi_{HD}(w,\hat{w},\hat{\theta}_n,\hat{V}_n,\hat{M}_{nn})=\delta\int_{t_1}^{t_2}\sum_e\left\{\frac{1}{2}\int_{A_e}D\left[\left(\frac{\partial^2 w}{\partial x^2}+\nu\frac{\partial^2 w}{\partial y^2}\right)\times\frac{\partial^2 w}{\partial x^2}+\left(\nu\frac{\partial^2 w}{\partial x^2}+\frac{\partial^2 w}{\partial y^2}\right)\frac{\partial^2 w}{\partial y^2}+\frac{1-\nu}{2}\times\left(2\frac{\partial^2 w}{\partial x\partial y}\right)^2\right]dA\right\}dt-\delta\int_{t_1}^{t_2}\sum_e\left\{\frac{1}{2}\int_{A_e}\rho\left(\frac{\partial w}{\partial t}\right)^2 dA\right\}dt+\int_{t_1}^{t_2}\sum_e\left\{\int_{A_e}p'\delta w\,dA\right\}dt+\delta\int_{t_1}^{t_2}\sum_e\left\{\int_{\partial A_e}\hat{V}_n(\hat{w}-w)-\hat{M}_{nn}\left(\hat{\theta}_n-\frac{\partial w}{\partial n}\right)dS\right\}dt=0 \tag{2}$$

In the above, A_e is the area of element e, ∂A_e the boundary of A_e, D the bending rigidity, ν Poisson's ratio, and ρ the mass per unit area of the panel. The element interior deflection w is a smooth function within A_e and need not satisfy the interelement compatibility requirements along ∂A_e a priori. The common interelement boundary deflection $\hat{w}$ is continuous on ∂A_e and satisfies the boundary conditions $\hat{w}=\bar{w}$ on Su_{e1}. The interelement boundary normal slope $\hat{\theta}_n$ is piecewise continuous on ∂A_e and satisfies the boundary condition $\hat{\theta}_n=\bar{\theta}_n$ on Su_{e2}. Su_{e1} and Su_{e2} are the portions of ∂A_e along which the deflection $\bar{w}$ and normal slope $\bar{\theta}_n$ are prescribed, respectively. $\hat{V}_n$ and $\hat{M}_{nn}$ serve as the Lagrangian multipliers on ∂A_e, and $\partial w/\partial n$ means the derivative of w in the normal direction.

In Eq. (2), Kirchhoff's hypotheses[24] for thin panels have been assumed and the rotational kinetic energy of the panel is neglected. Further, as seen in Eq. (2), no prescribed loadings, such as static pressure, boundary transverse shear, or bending moments, etc., are presented for the present flutter analysis.

Hence, the variational principle contains five time-dependent field variables, w, $\hat{w}$, $\hat{\Theta}_n$, $\hat{V}_n$, and $\hat{M}_{nn}$. By the variation of the functional $\delta\Pi_{HD}$, with respect to each of them, the stationary condition leads to the following Euler equations:

$$D\left(\frac{\partial^4 w}{\partial x^4}+2\frac{\partial^2 w}{\partial x^2\partial y^2}+\frac{\partial^4 w}{\partial y^4}\right)+\rho\frac{\partial^2 w}{\partial t^2}+p'=0 \quad \text{in } A_e \tag{3}$$

$$w=\hat{w} \quad \text{on } \partial A_e \tag{4}$$

$$\frac{\partial w}{\partial n}=\hat{\theta}_n \quad \text{on } \partial A_e \tag{5}$$

$$\frac{\partial}{\partial n}\left[-D\left(\frac{\partial^2 w}{\partial n^2}+\nu\frac{\partial^2 w}{\partial s^2}\right)\right]+2\frac{\partial}{\partial s}\left[-D(1-\nu)\frac{\partial^2 w}{\partial n\partial s}\right]=\hat{V}_n \quad \text{on } \partial A_e \tag{6}$$

$$-D\left(\frac{\partial^2 w}{\partial n^2}+\nu\frac{\partial^2 w}{\partial s^2}\right)=\hat{M}_{nn} \quad \text{on } \partial A_e \tag{7}$$

and natural boundary conditions

$$\hat{V}_n=0 \quad \text{on } S_{e_1} \tag{8}$$

$$\hat{M}_{nn}=0 \quad \text{on } S_{e_2} \tag{9}$$

As shown above, Eq. (3) is the equation of motion governing the flutter behavior of the thin cracked panel. From Eqs. (4) and (5), the compatibility requirements of the interelement deflection and its normal slope on ∂A_e are satisfied a posteriori. Equations (6-9) show that the Lagrangian multipliers $\hat{V}_n$ and $\hat{M}_{nn}$ are physically the equivalent transverse shear and bending moment on the interelement boundary ∂A_e, respectively, and thus the equilibrium conditions on the interelement boundary are satisfied a posteriori. Also, from Eqs. (8) and (9), the conditions of free equivalent transverse shear and free bending moment on the boundaries S_{e1} and S_{e2} are satisfied a posteriori.

Now, for the hybrid crack elements around the crack tip, the independent field variables w, $\hat{w}$, $\hat{\theta}_n$, $\hat{V}_n$, and $\hat{M}_{nn}$ can be assumed as follows:

$$w=e^{\Omega t}([U_R]\{\beta\}+[U_S]\{K_s\}) \tag{10}$$

$$\begin{Bmatrix}\hat{w}\\ \hat{\theta}_n\end{Bmatrix}=e^{\Omega t}[L]\{q\} \tag{11}$$

and

$$\begin{Bmatrix}\hat{V}_n\\ \hat{M}_{nn}\end{Bmatrix}=e^{\Omega t}[R]\{\alpha\} \tag{12}$$

Therefore,

$$\frac{\partial w}{\partial x}=e^{\Omega t}([U_{Rx}]\{\beta\}+[U_{Sx}]\{K_s\})$$

$$\frac{\partial w}{\partial y}=e^{\Omega t}([U_{Ry}]\{\beta\}+[U_{Sy}]\{K_s\})$$

and

$$\begin{Bmatrix}w\\ \frac{\partial w}{\partial n}\end{Bmatrix}=e^{\Omega t}([D_R]\{\beta\}+[D_S]\{K_s\})$$

In the above, Ω is the complex frequency of oscillation, $\{q\}$ the nondimensional nodal values, the column matrices $\{\alpha\}$ and $\{\beta\}$ are undetermined independent parameters, and $\{K_s\}$

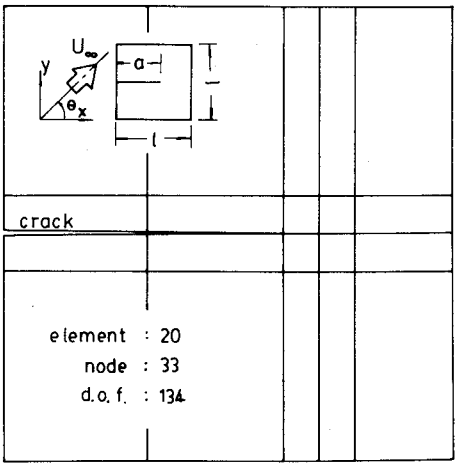

Fig. 1 Geometry and finite element mesh of a square cracked panel.

represents nondimensional bending stress intensity factors, say,

$$\{k_s\} = \frac{\ell^5}{D}\begin{Bmatrix} K_I \\ K_{II} \end{Bmatrix}$$

where ℓ denotes the characteristic length of the problem.

As mentioned previously, for simplicity, the remainder of the cracked panel is modeled by the conventional displacement finite element model for which the interelement compatibility conditions are satisfied a priori. Thus, the flutter response of the regular region of the cracked panel can be governed by $\delta\pi_{CD} = 0$, say,

$$\delta\pi_{CD}(w) = \delta\int_{t_1}^{t_2}\sum_e \left\{\frac{D}{2}\int_{A_e}\left(\frac{\partial^2 w}{\partial x^2}+\nu\frac{\partial^2 w}{\partial y^2}\right)\frac{\partial^2 w}{\partial x^2} + \left(\nu\frac{\partial^2 w}{\partial x^2}+\frac{\partial^2 w}{\partial y^2}\right)\frac{\partial^2 w}{\partial y^2}+\frac{1-\nu}{2}\left(2\frac{\partial^2 w}{\partial x\partial y}\right)^2 dA\right\}dt$$
$$-\delta\int_{t_1}^{t_2}\sum_e\left\{\frac{\rho}{2}\int_{A_e}\left(\frac{\partial w}{\partial t}\right)^2 dA\right\}dt + \int_{t_1}^{t_2}\sum_e\left\{\int_{A_e} p'\delta w dA\right\}dt \quad (13)$$

For regular conforming bending plate elements, the interpolation function of w can be assumed as

$$w = e^{\Omega t}[Z]\{q\} \quad (14)$$

Now, the variational principle of the whole thin cracked panel to be analyzed can be viewed as the sum of those in both regions. Hence,

$$\delta\pi = \delta\pi_{CD} + \delta\pi_{HD} = 0 \quad (15)$$

Based on Eq. (15), the relevant finite element formulations can then be carried out by substituting Eqs. (10-12), and (14) into Eq. (15), respectively. The final simultaneous homogeneous equations are shown here in advance:

$$([K^*] + \lambda[A^*] + g_d\Omega[A_d^*] + (\rho\ell^4/D)\Omega^2[M^*])\{q^*\} = \{0\} \quad (16)$$

where $[K^*]$, $[A^*]$, $[A_d^*]$, and $[M^*]$ represent the nondimensional global stiffness, aerodynamic, aerodynamic damping, and mass matrices, respectively. λ and g_d, which are known as the nondimensional dynamic pressure and the aerodynamic damping factor, are defined as

$$\lambda = \frac{2q_\infty \ell^3}{D\sqrt{M^2-1}}$$

and

$$g_d = \frac{1}{U_\infty}\frac{2q_\infty\ell^4}{D\sqrt{M^2-1}}\frac{M^2-2}{M^2-1}$$

To minimize the number of the total degrees of freedom at each node, the nodal variables are defined as (w, $\partial w/\partial x$, $\partial w/\partial y$, $\partial^2 w/\partial x\partial y$). Therefore, 16 degrees of freedom for each four-node conforming regular bending element are adopted. For the hybrid rectangular crack element, however, due to the Williams' behavior,[20] the second-order derivatives of the lateral displacement field do not exist at the crack tip. Thus, the nodal value $\partial^2 w/\partial x\partial y$ cannot be specified as one of the nodal variables at the crack tip. Consequently, the number of total degrees of freedom for the hybrid crack element is only 15.

Closely following the procedure of Chen and Chen,[17] the stiffness and mass matrices of the regular conforming bending elements and the hybrid rectangular crack bending elements can be easily derived, respectively, and, for brevity, are not shown here. Only the derivation of the aerodynamic and aerodynamic damping matrices is to be discussed in the next section.

Derivation of Aerodynamic Matrix $[A^*]$ and Aerodynamic Damping Matrix $[A_d^*]$

For singular bending elements, the aerodynamic term of the variational principle presented in Eq. (2) is

$$\delta V_{ah} = \int_{t_1}^{t_2}\sum_e\left\{\int_{A_e} p'\delta w dA\right\}dt \quad (17)$$

Substituting the interpolation functions of w, $\partial w/\partial x$, and $\partial w/\partial y$ into Eq. (17) and carrying out the integration over the time interval $[t_1, t_2]$, δV_{ah} is then nondimensionalized by the factor of ω_0/D as (ω_0 is the fundamental natural frequency of the cracked panel)

$$\frac{\omega_0}{D}\delta V_{ah} = \frac{\omega_0}{2\Omega}e^{2\Omega t}\Big|_{t_1}^{t_2}\sum_e\{\delta\beta\}^T(\lambda[\phi_1]+g_d\Omega[T_1])\{\beta\} + \{\delta\beta\}^T(\lambda[\Phi_2]+g_d\Omega[T_2])\{K_s\} + \{\delta K_s\}^T(\lambda[\Phi_4] + g_d\Omega[T_2]^T)\{\beta\} + \{\delta K_s\}^T(\lambda[\Phi_3]+g_d\Omega[T_3])\{K_s\} \quad (18)$$

where $[\ ]^T$ is the transverse of $[\ ]$,

$$[T_1] = \frac{1}{\ell^4}\int_{A_e}[U_R]^T[U_R]dA$$

$$[T_2] = \frac{1}{\ell^4}\int_{A_e}[U_R]^T[U_S]dA$$

$$[T_3] = \frac{1}{\ell^4}\int_{A_e}[U_S]^T[U_S]dA$$

$$[\Phi_1] = \frac{1}{\ell^3}\int_{A_e}\cos\theta[U_R]^T[U_{Rx}] + \sin\theta[U_R]^T[U_{Ry}]dA$$

$$[\Phi_2] = \frac{1}{\ell^3}\int_{A_e}\cos\theta[U_R]^T[U_{Sx}] + \sin\theta[U_R]^T[U_{Sy}]dA$$

$$[\Phi_3] = \frac{1}{\ell^3}\int_{A_e}\cos\theta[U_S]^T[U_{Sx}] + \sin\theta[U_S]^T[U_{Sy}]dA$$

$$[\Phi_4] = \frac{1}{\ell^3}\int_{A_e}\cos\theta[U_S]^T[U_{Rx}] + \sin\theta[U_S]^T[U_{Ry}]dA$$

Since $\{\alpha\}$ and $\{\beta\}$ are independent for each singular element, as proved by Chen and Chen,[17] one obtains

$$\{\beta\} = [P_1]^{-1}[G]\{q\} - [P_1]^{-1}[P_2]\{K_s\} \quad (19)$$

where $[\ ]^{-1}$ is the inverse of $[\ ]$,

$$[P_1] = \int_{\partial A_e}[R]^T[D_R]dS$$

$$[P_2] = \int_{\partial A_e}[R]^T[D_S]dS$$

$$[G] = \int_{\partial A_e}[R]^T[L]dS$$

Substituting Eq. (19) into Eq. (18), it can be expressed as

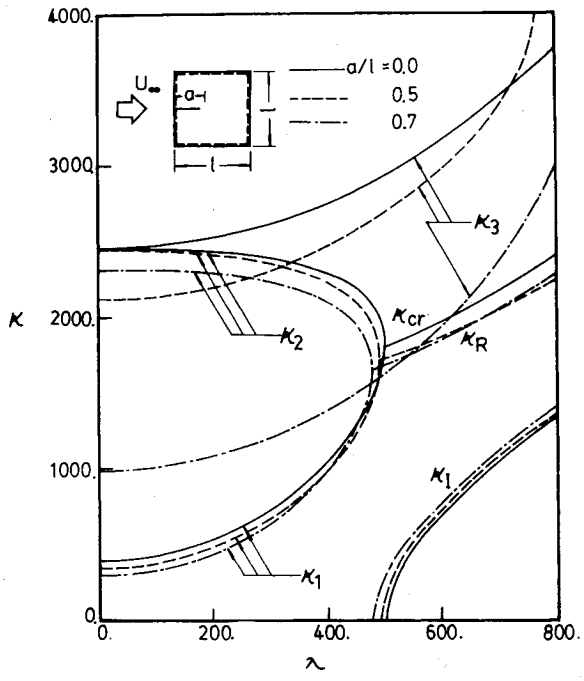

Fig. 2 Variations of nondimensional eigenvalues κ vs nondimensional dynamic pressure λ of a simply supported edge-cracked panel in a normal flow.

$$\frac{\omega_0}{D}\delta V_{ah}=\frac{\omega_0}{2\Omega}e^{2\Omega t}\Big|_{t_1}^{t_2}\sum_e\{\delta q\}^T(\lambda[A_1]+g_d\Omega[A_{d_1}])\{q\}$$
$$+\{\delta q\}^T(\lambda[A_2]+g_d\Omega[A_{d_2}])\{K_s\}+\{\delta K_s\}^T(\lambda[A_4]$$
$$+g_d\Omega[A_{d_2}]^T)\{q\}+\{\delta K_s\}^T(\lambda[A_3]+g_d\Omega[A_{d_3}])\{K_s\} \tag{20}$$

in which

$$[A_{d_1}]=[G]^T[P_1]^{-T}[T_1][P_1]^{-1}[G]$$
$$[A_{d_2}]=[G]^T[P_1]^{-T}([T_2]-[T_1][P_1]^{-1}[P_2])$$
$$[A_{d_3}]=[T_3]+[P_2]^T[P_1]^{-T}([T_1][P_1]^{-1}[P_2]-2[T_2])$$
$$[A_1]=[G]^T[P_1]^{-T}[\Phi_1][P_1]^{-1}[G]$$
$$[A_2]=[G]^T[P_1]^{-T}([\Phi_2]-[\Phi_1][P_1]^{-1}[P_2])$$
$$[A_3]=[\Phi_3]+[P_2]^T[P_1]^{-T}[\Phi_1][P_1]^{-1}[P_2]$$
$$-[\Phi_4][P_1]^{-1}[P_2]-[P_2]^T[P_1]^{-T}[\Phi_2]$$

and

$$[A_4]=([\Phi_4]-[P_2]^T[P_1]^{-T}[\Phi_1])[P_1]^{-1}[G]$$

Define

$$[A_h]=\begin{bmatrix}[A_1] & [A_2]\\ [A_4] & [A_3]\end{bmatrix},\quad [A_{dh}]=\begin{bmatrix}[A_{d_1}] & [A_{d_2}]\\ [A_{d_2}] & [A_{d_3}]\end{bmatrix}$$

and

$$\{q_h\}=\begin{Bmatrix}\{q\}\\ \{K_s\}\end{Bmatrix}$$

Equation (20) can be rewritten as

$$\frac{\omega_0}{D}\delta V_{ah}=\frac{\omega_0}{2\Omega}e^{2\Omega t}\Big|_{t_1}^{t_2}\sum_e\{\delta q_h\}^T(\lambda[A_h]+g_d\Omega[A_{dh}])\{q_h\}$$

Here, $[A_h]$ and $[A_{dh}]$ represent the nondimensional aerodynamic and aerodynamic damping matrices of singular bending elements, respectively.

For regular elements, a similar procedure is performed. The result can be quoted as

$$\frac{\omega_0}{D}\delta V_{ac}=\frac{\omega_0}{2\Omega}e^{2\Omega t}\Big|_{t_1}^{t_2}\sum_e\{\delta q\}^T(\lambda[A_c]+g_d\Omega[A_{dc}])\{q\}$$

where

$$[A_c]=\frac{l}{\ell^3}\int_{A_e}\cos\theta[Z]^T[Z_x]+\sin\theta[Z]^T[Z_y]\,dA$$

and

$$[A_{dc}]=\frac{l}{\ell^4}\int_{A_e}[Z]^T[Z]\,dA$$

Again, $[A_c]$ and $[A_{dc}]$ represent the nondimensional aerodynamic and aerodynamic damping matrices of regular bending elements, respectively.

Now, the aerodynamic energy δV_a exerted on the cracked panel can be obtained by the sum of δV_{ah} and δV_{ac} such that

$$\frac{\omega_0}{D}\delta V_a=\frac{\omega_0}{D}\delta V_{ah}+\frac{\omega_0}{D}\delta V_{ac}$$
$$=\frac{\omega_0}{2\Omega}e^{2\Omega t}\Big|_{t_1}^{t_2}\{\delta q^*\}^T(\lambda[A^*]+g_d\Omega[A_d^*])\{q^*\}$$

where $[A^*]$, $[A_d^*]$, and $\{q^*\}$ are the global nondimensional aerodynamic, aerodynamic damping, and nodal value matrices assembled from the corresponding element properties.

Solution Technique for the Eigensystem

In solving the simultaneous homogeneous equation [Eq. (16)], it is found that the nondimensional aerodynamic damping matrix $[A_d^*]$ derived is equal to the nondimensional mass matrix $[M^*]$ which can be found in Ref. 17. Hence, for simplicity, Eq. (16) can be rewritten as

$$([K^*]+\lambda[A^*]-\kappa[M^*])\{q^*\}=\{0\} \tag{21}$$

where

$$\kappa=-(\rho\ell^4/D)\Omega^2-g_d\Omega \tag{22}$$

and the flutter problem leaves itself to the determination of the eigenvalues κ and associated eigenvectors $\{q^*\}$.

However, due to the unsymmetric nature of the aerodynamic matrix $[A^*]$, the numerical analysis of flutter problems usually involves solving a large eigensystem and the reduction of the size of the system is imperative. For this purpose, Rossettos and Tong[6] proposed thd modal method for which only several modes of natural vibration are chosen to represent the eigenvectors of the flutter problem, and the accuracy of the solution is still maintained. Thus, the reduction of the size of the eigensystem is achieved. The same procedure is also employed in this work before the use of the QR algorithm[21] to calculate the eigenvalues and eigenvectors.

Conditions of Stability and Instability

As seen in the preceding section, once the nondimensional dynamic pressure λ is specified, the eigenvalues κ and associated eigenvectors $\{q^*\}$ can be solved. It should be noted that both matrices $[K^*]$ and $[M^*]$ are positive definite, whereas $[A^*]$ is unsymmetric in nature. If $\lambda=0$, positive eigenvalues and real eigenvectors are obtained provided that the cracked panel is well constrained. As λ increases from zero monotonically, the mode shapes (or eigenvectors) are then distorted by the aerodynamic pressure, and complex or negative eigenvalues may be found.

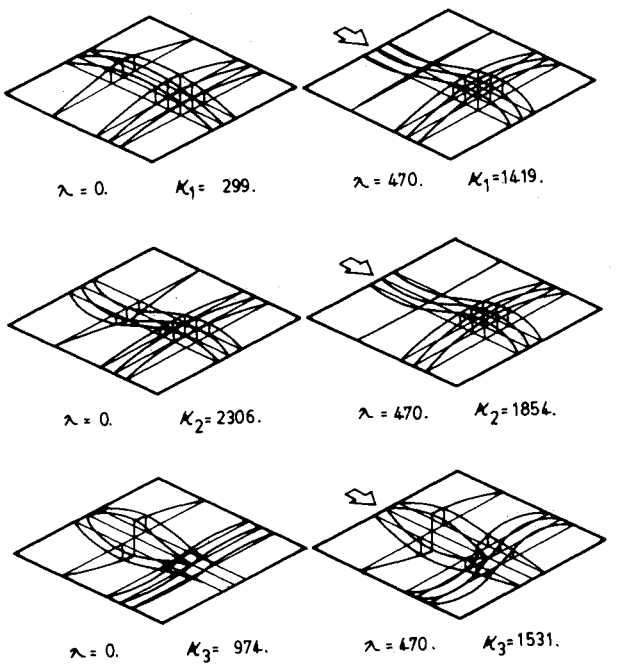

Fig. 3 The mode shapes of κ_1, κ_2, and κ_3 of a simply supported edge-cracked panel with $a/\ell = 0.7$ in a normal flow at $\lambda = 0.0$ and 470.0, respectively.

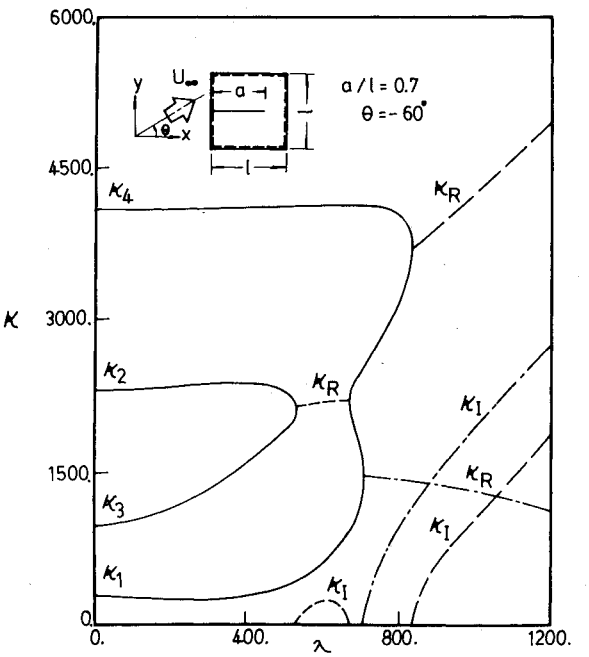

Fig. 4 Variations of nondimensional eigenvalues κ vs nondimensional dynamic pressure λ of a simply supported edge-cracked panel with $a/\ell = 0.7$ in a yawed flow with $\theta = -60$ deg.

It is well known that the stability of a structure is dominated by the real parts of the complex frequencies. If, and only if, one of them is positive, the structure is unstable. From Eq. (22), two roots of the complex frequency Ω can be yielded once the corresponding eigenvalues κ of the system are evaluated from Eq. (21). The result is

$$\Omega/\omega_0 = \tfrac{1}{2}\left[-B \pm \{B^2 - (4\kappa/\kappa_0)\}^{1/2}\right] \tag{23}$$

Here,

$$B = g_d D/\rho \ell^4 \omega_0 \quad \text{and} \quad \kappa_0 = \rho \ell^4 \omega_0^2 / D$$

represents the nondimensional aerodynamic damping factor and the fundamental eigenvalue of natural vibration.

Since $B \geq 0$, the real parts of the two roots of Ω/ω_0 are negative whenever $\kappa > 0$, and one of them becomes positive when $\kappa < 0$. In the latter case, the panel is unstable and the fluttering instability is of a divergent type.[22,23] For the complex eigenvalue κ and frequency Ω, say, $\kappa = \kappa_R + i\kappa_I$ and $\Omega = \Omega_R + i\Omega_I$, it is shown that

$$\left(B^2 - \frac{4\kappa}{\kappa_0}\right)^{1/2} = \pm\sqrt{A}e^{i(\phi/2)}$$

and

$$\frac{\Omega_R}{\omega_0} = \frac{1}{2}\left(-B \pm \sqrt{A}\cos\frac{\phi}{2}\right)$$

where $-\pi < \phi < \pi$, and

$$A = \left[\left(B^2 - \frac{4\kappa_R}{\kappa_0}\right)^2 + \left(\frac{4\kappa_I}{\kappa_0}\right)^2\right]^{1/2}$$

$$\cos\phi = \frac{1}{A}\left(B^2 - \frac{4\kappa_R}{\kappa_0}\right), \quad \sin\phi = \frac{1}{A}\left(-\frac{4\kappa_I}{\kappa_0}\right)$$

Since $\cos(\phi/2) > 0$, the condition of positive Ω_R is

$$\sqrt{A}\cos(\phi/2) > B$$

or, equivalently,

$$\left(\frac{\kappa_I}{\kappa_0}\right)^2 > B^2\frac{\kappa_R}{\kappa_0} \tag{24}$$

Thus, once $|\kappa_I|$ is large enough, the panel may be unstable. In addition, when the eigenvalue becomes complex, so does the corresponding eigenvector. Physically, the complex eigenvector implies the out-of-phase oscillation and provides the possibility of the fluttering instability of oscillatory type.

Results and Discussions

The geometric configuration considered in the numerical examples is a thin square panel with an edge crack of length a whose optimum finite element mesh is shown in Fig. 1. Four 15-degree-of-freedom rectangular singular bending elements are surrounded by four-node conforming regular bending elements.[17] Fifteen modes of natural vibration are chosen and employed in the present modal method to reduce the size of the eigensystem. The material is assumed to be isotropic with Poisson's ratio $\nu = 0.3$.

The accuracy of the analysis procedure developed is first tested by studying the flutter response of noncracked panels. Three cases of different boundary conditions are investigated: 1) simply supported conditions with a normal flow, 2) simply supported conditions with a yawed flow of $\theta = -60$ deg, and 3) a cantilever condition with a normal flow. The variation between the computed nondimensional critical dynamic pressure λ_{cr} and those available in literature[3,5,6] is within 2%.

As seen in Fig. 2, a simply supported edge-cracked panel is immersed in a normal supersonic flow, and three eigenvalues denoted by κ_1, κ_2, and κ_3 as shown are presented. As λ increases from zero monotonically, κ_1 and κ_2 approach each other and coalesce at a critical value, say κ_{cr}, which corresponds to the value of λ_{cr}. If $\lambda < \lambda_{cr}$, the cracked panel is stable and fluttering instability does not occur. When λ increases further from λ_{cr}, however, κ_1 and κ_2 becomes a complex conjugate pair and the oscillatory-type fluttering instability can be expected. It is observed from Fig. 2 that the values of λ_{cr} and κ_{cr} are only lightly affected by the existence of cracks for the case of simply supported panels subjected to a normal flow. In addition, for the case of $a/\ell = 0.5$, it is in-

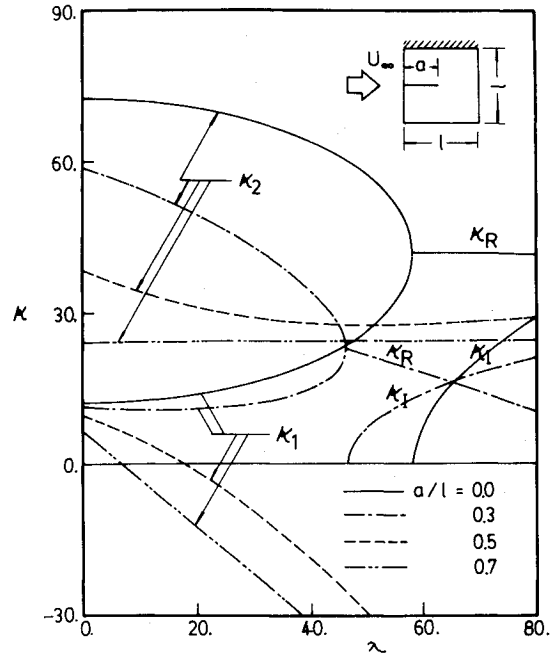

Fig. 5 Variations of nondimensional eigenvalues κ vs nondimensional dynamic pressure λ of a cantilever edge-cracked panel in a normal flow.

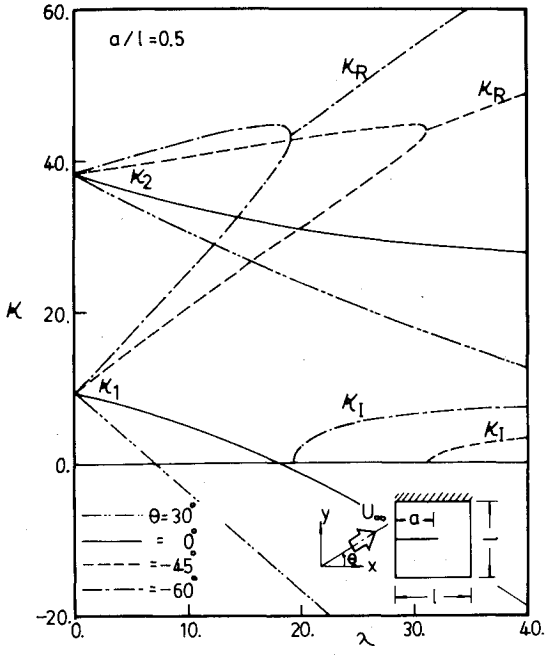

Fig. 6 Variations of nondimensional eigenvalues κ vs nondimensional dynamic pressure λ of a cantilever edge-cracked panel with $a/\ell = 0.5$ in various yawed flows using hybrid crack elements.

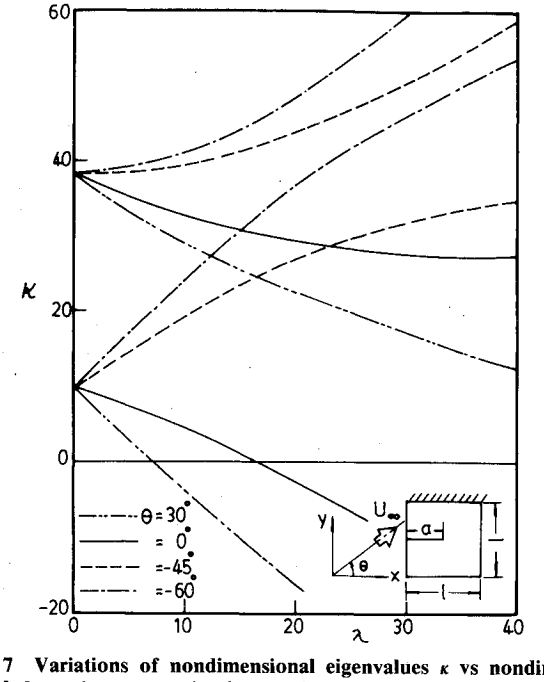

Fig. 7 Variations of nondimensional eigenvalues κ vs nondimensional dynamic pressure λ of a cantilever edge-cracked panel with $a/\ell = 0.5$ in various yawed flows using regular crack elements.

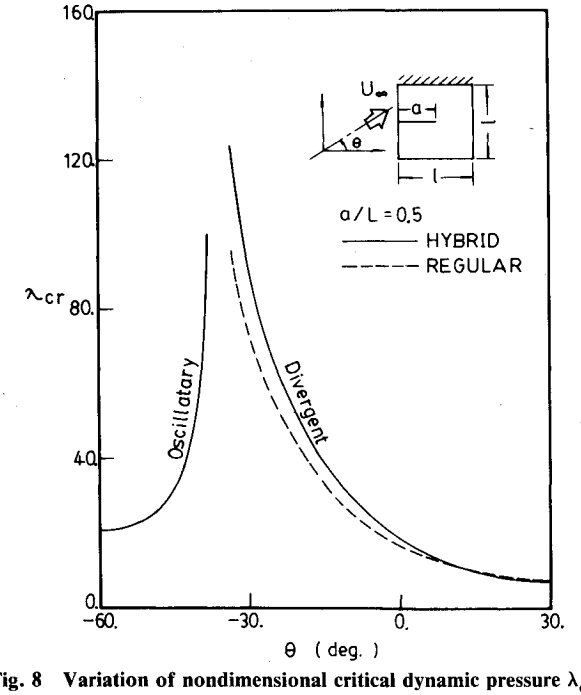

Fig. 8 Variation of nondimensional critical dynamic pressure λ_{cr} vs the direction angles of yawed flows for a cantilever edge-cracked panel with $a/\ell = 0.5$.

teresting to note that κ_2 and κ_3 intersect with each other before the coalescence of κ_1 and κ_2. A similar phenomenon also takes place for κ_1 and κ_3 when $a/\ell = 0.7$. Since those intersections do not bring complex conjugate roots of κ, such a phenomenon only suggests the possibility of selecting the coalescing modes, and may be interpreted as follows: For example, for the case of $a/\ell = 0.7$ as seen in Fig. 3, the mode shapes of κ_1 and κ_2 are symmetric with respect to the line of crack, however, the mode shape of κ_3 is antisymmetric. Thus, the coalescence between modes κ_1 and κ_3 is hardly expected.

Variations of eigenvalues κ vs the nondimensional aerodynamic pressure for the yawed supersonic flow with $\theta = -60$ deg are shown in Fig. 4. As displayed in Fig. 4, the regions of preliminary coalescence of κ_2 an κ_3 are found. According to the instability condition as expressed in Eq. (24), the region of preliminary coalescence may remain stable if the nondimensional aerodynamic damping factor B is large enough. This may provide the idea to shift the critical speed to a higher value by increasing the damping effects of the system.

As shown in Fig. 5, a cantilever edge-cracked panel is immersed in a normal supersonic flow, and the eigenvalues of κ_1 for cases $a/\ell = 0.5$ and 0.7 do not intersect with the corresponding eigenvalues of κ_2. When those eigenvalues decrease to negative values, the divergent-type fluttering instability occurs. These are of practical importance for the safety design of

aeronautical structures. Further, the significant influence of the crack length on the determination of λ_{cr} can be found.

In addition to the significant influence of crack length, the flow direction also plays an important role in determining the type of fluttering instability as shown in Fig. 6 for the case of $a/\ell=0.5$. It is seen that the fluttering instability is of oscillatory type as $\theta=-60$ and -45 deg while it changes to the divergent type as $\theta=0$ and 30 deg. To assess the necessity of using hybrid crack elements, the same problem is also carried out using the conforming regular elements only. As shown in Fig. 7, a different scheme of fluttering instability is predicted, especially as $\theta=-60$ and -45 deg. Figure 8 displays the variations of λ_{cr} vs the direction angles for the case of $a/\ell=0.5$. It is found that the oscillatory and divergent types of fluttering instability are demarcated at $\theta\sim-38$ deg. It is worthwhile to note that the angle of demarcation corresponds to the highest critical speed, and, therefore, has the best ability to resist the occurrence of stability. For comparison purposes, the results obtained using regular crack elements are also drawn. Again, no oscillatory types of fluttering instability can be found.

Concluding Remarks

As assumed hybrid-displacement finite element model has been presented successfully to deal with various flutter problems of thin cracked panels. The effects of flow direction and the changes between types of fluttering instability are studied. It is found that the existence of cracks decreases the critical speed, and, hence, weakens the resistance of cracked panels to flutter. The demarcation between oscillatory and divergent types of fluttering instability usually corresponds to the highest critical speed, if no other effects are involved. Further, the importance of the aerodynamic damping effect is observed in cases of oscillatory-type instability. Finally, the necessity of using hybrid crack elements in dealing with the flutter problems of thin cracked panels is also demonstrated. The computer program devised in this work can be extended further to treat the nonlinear flutter problems in which the in-plane forces induced by large deflections of the panel are considered, and will be presented in a subsequent report.

References

[1]Ashley, H. and Zartarian, G., "Piston Theory—A New Aerodynamic Tool for the Aeroelastician," *Journal of the Aeronautical Sciences*, Vol. 23, Dec. 1956, pp. 1109-1118.

[2]Olson, M. D., "Finite Elements Applied to Panel Flutter," *AIAA Journal*, Vol. 5, Dec. 1967, pp. 2267-2270.

[3]Olson, M. D., "Some Flutter Solutions Using Finite Elements," *AIAA Journal*, Vol. 8, April 1970, pp. 747-752.

[4]Kariappa, Somasheker, B R., and Shah, C. G., "Discrete Element Approach to Flutter of Skew Panels with Inplane Forces under Yawed Supersonic Flow," *AIAA Journal*, Vol. 8, Nov. 1970, pp. 2017-2022.

[5]Sander, G., Bon, C., and Geradin, M., "Finite Element Analysis of Supersonic Panel Flutter," *International Journal for Numerical Methods in Engineering*, Vol. 7, No. 3, 1973, pp. 379-394.

[6]Rossettos, J. N. and Tong, P., "Finite-Element Analysis of Vibration and Flutter of Cantilever Anisotropic Plates," *Transactions of ASME Journal of Applied Mechanics*, Vol. 41, Dec. 1974, pp. 1075-1080.

[7]Sawyer, J. W., "Flutter and Buckling of General Laminated Plates," *Journal of Aircraft*, Vol. 4, April 1977, pp. 387-393.

[8]Fung, Y. C., "On Two-Dimensional Panel Flutter," *Journal of Aeronautical Sciences*, Vol. 25, No. 3, 1958, pp. 145-160.

[9]Dowell, E. H. and Voss, H. M., "Theoretical and Experimental Panel Flutter Studies in the Mach Number Range 1.0 to 5.0," *AIAA Journal*, Vol. 3, Dec. 1965, pp. 2292-2304.

[10]Dowell, E. H., "Nonlinear Oscillations of a Fluttering Plate," *AIAA Journal*, Vol. 4, July 1966, pp. 1267-1275.

[11]Chen, W. H. and Huang, Y. H., "Fracture Mechanics Investigations of Rotating Disks with Cracks," *Journal of the Chinese Society of Mechanical Engineers*, Vol. 1, No. 1, 1980, pp. 21-32.

[12]Chen, W. H. and Wang, C. H., "An Assumed Hybrid Displacement Finite Element Model for Elastodynamic Cracked Problems," *Engineering Structures*, Vol. 3, No. 4, 1981, pp. 249-255.

[13]Chen, W. H. and Huang, Y. H., "An Elastodynamic Finite Element Procedure for Fracture Mechanics Investigations of Rotating Disks," Fifth International Conference on Fracture, Cannes, France, April 1981.

[14]Chen, W. H. and Wu, C. W., "On Elastodynamic Fracture Mechanics Analysis of Bimaterial Structures Using Finite Element Method," *Engineering Fracture Mechanics*, Vol. 15, No. 1-2, 1981, pp. 155-168.

[15]Chen, W. H. and Lin, T. C., "A Mixed-Mode Crack Analysis of Rotating Disk Using Finite Element Method," *Engineering Fracture Mechanics*, Vol. 17, No. 1, 1983, pp. 133-143.

[16]Chen, W. H., "Some Recent Researches on Fracture Mechanics Analysis in Tsing Hua University," *Proceedings of the ROC-ROK Joint Workshop on Fracture of Metals*, Seoul, Korea, April 1983, pp. 217-240.

[17]Chen, W. H. and Chen, P. Y., "A Hybrid-Displacement Finite Element Model for the Bending Analysis of Thin Cracked Plates," *International Journal of Fracture*, Vol. 24, No. 2, 1984, pp. 83-106.

[18]Barsoum, R. S., "Finite Element Method Applied to the Problem of Stability of a Non-conservative System," *International Journal for Numerical Methods in Engineering*, Vol. 3, No. 1, 1971, pp. 63-87.

[19]Tong, P., "New Displacement Hybrid Finite Element Models for Solid Continua," *International Journal for Numerical Methods in Engineering*, Vol. 2, No. 1, 1970, pp. 73-84.

[20]Williams, M. L., "The Bending Stress Distribution at the Base of a Stationary Crack," *Transactions of ASME, Journal of Applied Mechanics*, Vol. 28, No. 1, 1961, pp. 78-82.

[21]Wilkinson, J. H., *The Algebraic Eigenvalue Problem*, Clarendon Press, Oxford, 1965, Chap. 8.

[22]Fung, Y. C., *The Theory of Aeroelasticity*, Dover, New York, 1968, Chap. 6.

[23]Shanthakumar, P., Nagaraj, V. T., and Narayama Raju, P., "Influence of Support Location on Panel Flutter," *Journal of Sound and Vibration*, Vol. 53, No. 2, 1977, pp. 273-281.

[24]Ugural, A. C., *Stresses in Plates and Shells*, McGraw-Hill Book Co., New York, 1981, pp. 2,3.